nature protocols

PROTOCOL

https://doi.org/10.1038/s41596-019-0215-x

Real-time visualization of mutations and their fitness effects in single bacteria

Lydia Robert[1,2*], Jean Ollion[1] and Marina Elez[1,3*]

Mutations are the driving force of evolution and the source of important pathologies. The characterization of the dynamics and effects of mutations on fitness is therefore central to our understanding of evolution and to human health. This protocol describes how to implement two methods that we recently developed: mutation visualization (MV) and microfluidic mutation accumulation (μMA), which allow the occurrence of mutations created by DNA replication errors (MV) and the evolution of cell fitness during MA (μMA) to be followed directly in individual cells of *Escherichia coli*. MV provides a quantitative characterization of the dynamics of mutation occurrences, and μMA allows precise estimation of the distribution of fitness effects (DFEs) of mutations. Both methods use microfluidics and time-lapse microscopy, and a fluorescent mismatch repair (MMR) MutL protein is used as a marker for nascent mutations. Here, we present a single protocol describing how to implement the MV and μMA methods, including detailed procedures for microfluidic setup installation, data acquisition and data analysis and interpretation. Using this procedure, the microfluidic setup installation can be completed within 1 d, and automated data acquisition takes 2–4 d.

Introduction

In recent years, the development of new tools has enabled a growing number of cellular processes to be studied at the single-cell level. This has allowed the sometimes striking diversity between isogenic individuals to be deciphered. However, one important cellular process that remained beyond the reach of single-cell studies until recently was mutagenesis, that is, the generation of DNA mutations. Until recently there was no tool available that could detect mutations and assess their effects directly, at the single-cell level. Mutations are a major cause of diversity among organisms and play an important role in human diseases such as cancer. Therefore, the capacity to characterize mutagenesis at the single-cell level has important implications for the study of evolution and pathological cell physiology.

Here, we describe a protocol to implement our recently described method[1] for characterization of mutagenesis at the single-cell level.

Other methods for characterization of mutagenesis

Mutations have mainly been studied using two methods. The first one, the fluctuation test[2], is widely used to measure the mutation rate in various cell types. It is an indirect method that reveals selectable mutants arising during the growth of a population, by plating cells on a selective medium[3]. In this approach, the estimation of the mutation rate relies on several assumptions that may not be realized during experiments[3]. Mutation rates obtained by this approach can thus be substantially biased[4]. In addition, the mutations that can be detected by a fluctuation test typically arise at a single genetic locus corresponding to the selectable phenotype. The rate estimated from this locus might not reflect the rate at the whole-genome scale, due for instance, to differences in base composition or transcriptional activity between different loci[5].

The second widely used method to study mutations, the MA assay, was initially intended to characterize the effects of mutations on an organism's fitness, that is, on its ability to survive and reproduce[6]. The principle of this assay is to follow the temporal evolution of the fitness of organisms or cells as they accumulate mutations in the absence of natural selection. In practice, initially isogenic lines of individuals are propagated and accumulate mutations for many generations, whereas natural

[1]Laboratoire Jean Perrin, UMR 8237, CNRS, Sorbonne Universités, UPMC Université Paris 06, Paris, France. [2]Micalis Institute, Institut National de la Recherche Agronomique, AgroParisTech, Université Paris-Saclay, Jouy-en-Josas, France. [3]Institute of Systems and Synthetic Biology, UMR 8030, CNRS, Commissariat à l'Energie Atomique et aux Energies Alternatives, Genopole, Université d'Evry Val-d'Essonne, Université Paris Saclay, Evry, France. *e-mail: lydia.robert@upmc.fr; marina.elez@upmc.fr

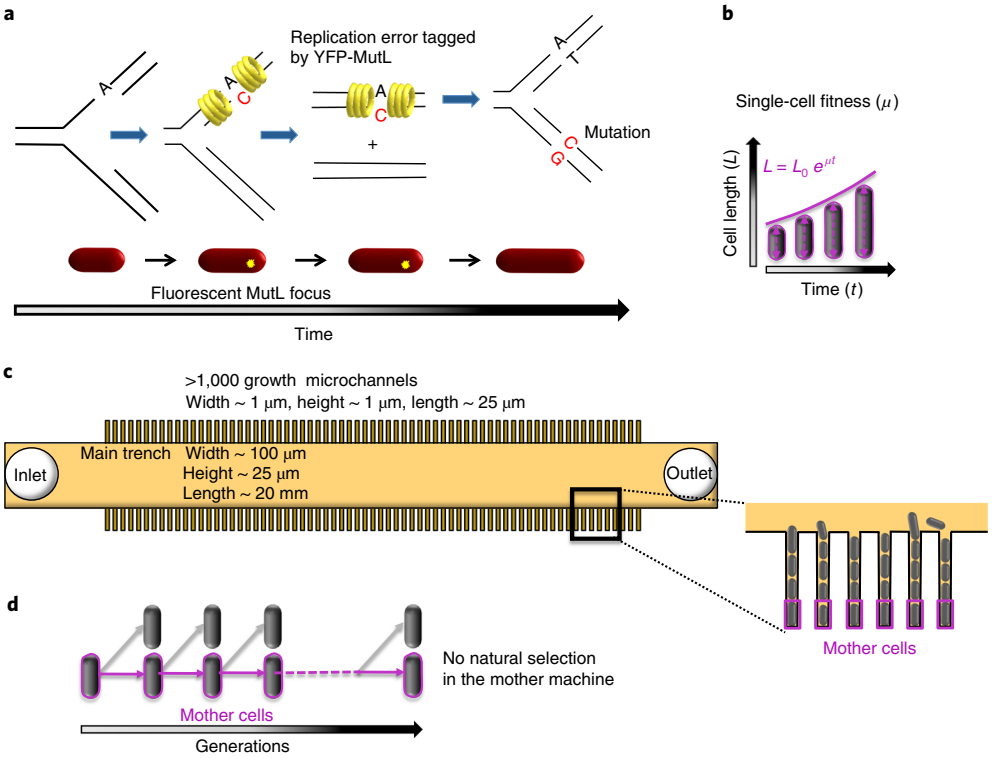

Fig. 1 | Principles of MV and μMA experiments in *E. coli*. **a**, Visualization of mutations caused by replication errors in *E. coli*. YFP-MutL accumulates on DNA around replication errors, creating a fluorescent focus. When errors are not repaired, the focus lasts until a new round of DNA replication fixes the mutation in one of the two DNA molecules. **b**, Malthusian fitness can be defined at the single-cell level as the elongation rate. **c**, Design of the mother machine microfluidic chip used for MV and μMA experiments. **d**, The mother machine allows the mother cell at each division to be retained. This device therefore implements a perfect bottleneck, where only one cell is kept at each generation, independently of its fitness, thus eliminating natural selection.

selection is limited by frequent population bottlenecks during which the population is reduced to one or a few individuals. Initially, both the mutation rate and the effects of mutations were estimated from the fitness evolution, which precluded the quantitative estimation of the DFEs of mutations[7,8]. However, in some recent MA assays, the mutation rate is estimated independently of the fitness measurements through whole-genome sequencing of the MA lines (MA-WGS)[9]. Still, the precision of DFE estimation using the MA-WGS approach is limited by the small number of independent lines that can be followed. In addition, in microorganisms, natural selection acts during the cycles of population growth and purges strongly deleterious and lethal mutations, thus biasing the mutation sample. This represents an issue both for the estimation of the DFE and for the estimation of the mutation rate by MA-WGS.

Finally, both MA-WGS and fluctuation tests estimate mutation rates at the population level, thus overlooking single-cell variability.

Development of the protocol

To investigate the occurrences and effects of mutations directly at the single-cell level, we recently developed two methods based on microfluidics, time-lapse imaging and a fluorescent tag of the MMR system in *E. coli*[1]. The first method, which we call MV, enables the detection of mutations arising from replication errors in real time in individual living cells. Mutation detection is based on the expression of an MMR protein that is fluorescently tagged with yellow fluorescent protein (YFP-MutL)[10], which accumulates on DNA mismatches created by replication errors, thus producing a fluorescent spot inside the cell. MutL foci corresponding to errors that are successfully repaired by MMR are short lived. By contrast, MutL foci–tagging replication errors that MMR fails to repair, that is, nascent mutations, last until the next round of replication converts the DNA mismatch into a mutation (Fig. 1a). Therefore, nascent mutations generate MutL foci with a lifetime of one doubling

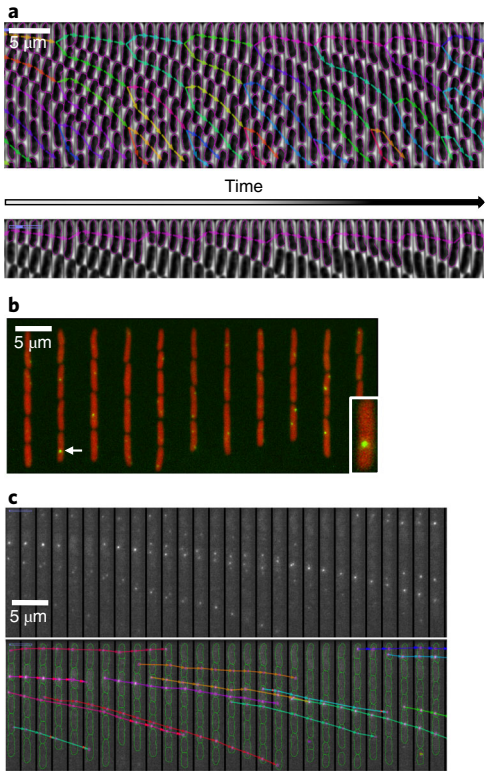

Fig. 2 | MV and µMA experiments in *E. coli*. a, Images from a typical µMA experiment. Top: kymograph of a single microchannel through time, imaged in phase contrast. Image analysis was performed using our BACMMAN software. Cell contours obtained with BACMMAN are shown in magenta, and tracking is shown with colored arrows. Bottom: same kymograph, showing the lineage of the mother cells. **b**, Image from a typical MV experiment with a strain expressing tdCherry and YFP-MutL. Overlay of red fluorescence and yellow fluorescence images. The arrow indicates a YFP-MutL focus, that is, a nascent mutation, and the inset contains a magnified image of this focus. **c**, Kymograph of a single microchannel through time, imaged in yellow fluorescence in a typical MV experiment. Fluorescent foci indicate nascent mutations. The bottom panel presents the analysis performed by our BACMMAN software. Cells are segmented (green contours). Fluorescent foci are segmented (magenta contours) and tracked (colored arrows).

time, for instance, ~20 min for a wild-type *E. coli* strain in Luria-Bertani (LB) medium. The second method, which we call µMA, allows the fitness of single cells during MA to be followed in the absence of natural selection. Malthusian fitness, which is defined at the population level as the exponential rate of biomass increase, can be measured at the single-cell level as the elongation rate, because *E. coli* cells elongate exponentially from birth to division (Fig. 1b).

To achieve precise control of the environment and high-throughput single-cell data acquisition in MV and µMA, we use a microfluidic chip called the 'mother machine'[11]. The mother machine contains thousands of narrow microchannels in which cells grow in single file (Fig. 1c). These microchannels are closed at one end and open at the other end onto a bigger channel where the growth medium flows (Fig. 1c). The geometry of the growth microchannels allows the 'mother' cell abutting the dead end to be retained, irrespectively of whether it grows faster or more slowly than the other cells in the microchannel (Fig. 1d). This completely blocks natural selection and allows all mutations that arise during growth to be accessed, including very deleterious and lethal mutations. This is particularly important for the estimation of the DFE, which requires an unbiased sample of mutations.

In the µMA experiments described in Robert et al.[1], cells are imaged in phase contrast every 4 min, for 24–72 h, corresponding to up to 200 cell divisions (Fig. 2a). Growth rate, that is, fitness, can be measured at each generation for more than a thousand mother cells in parallel, thus generating $>10^5$ fitness measurements per experiment. In the MV experiments described in Robert et al.[1], cells expressing a constitutive red fluorescence and a yellow YFP-MutL protein for mutation detection are imaged in the two corresponding fluorescence channels (Fig. 2b). Images are taken every 2 min for 24–72 h. This allows the detection and tracking of hundreds to thousands (depending on the strain's

mutation rate) of fluorescent MutL spots—the nascent mutations—in mother cells. Long-term imaging of cells in MV and μMA produces a large amount of data. Analyzing MV and μMA data thus requires fast and reliable software for automated image analysis. We therefore developed such software, which we called BACMMAN[1]. Details of BACMANN's functionalities and the different analysis procedures it enables are given in the accompanying protocol[12]. In brief, BACMMAN has the ability to detect, segment and track bacteria growing in the mother machine from either phase-contrast or fluorescence images and to detect and track intracellular fluorescent spots (Fig. 2a,c). It includes an intuitive user interface designed to efficiently visualize massive datasets and perform interactively semi-automatic corrections of segmentation and lineage results. A coupling to data analysis software allows the focus of semi-automatic intervention on subsets of data with specific properties.

Applications of the method

In Robert et al.[1], μMA experiments were performed in rich medium, using bacterial strains that are well adapted to their growth conditions. μMA experiments performed using various suboptimal genotypes would allow investigation of how the DFE changes as a function of the initial adaptation level and would also offer a way to characterize epistasis. Interestingly, the occurrence of beneficial mutations may be observed in this case. Our approach could also be used to follow the dynamics of mutations and the effects of mutations on fitness in other growth conditions, particularly in stressful environments. The use of microfluidics in both MV and μMA also allows mutation incidence and fitness trajectories to be followed in controlled, fluctuating environments.

Although this protocol was developed to follow mutation dynamics and fitness effects in *E. coli* cells growing in rich LB medium, as described in Robert et al.[1], it is directly applicable to other growth media. In addition, the protocol that we present here could easily be adapted to perform μMA in stressful conditions, such as during exposure to ultraviolet light (UV) or to different drugs such as xenobiotics or antibiotics. Note, however, that conditions inducing high mortality will limit the time scale of the experiment and may consequently deteriorate or even prevent the estimation of fitness effects. MV experiments can also be performed in stressful conditions using our protocol. Interestingly, Uphoff[13] recently performed similar MV experiments to follow the increase in DNA replication error rate following treatment with the DNA alkylating agent methyl methane sulfonate. However, care should be taken when applying external stress to the cells, because these treatments could induce protein aggregation, leading to fluorescent MutL aggregates that could be mistakenly interpreted as replication errors. Therefore, our advice is to systematically check, for each new experimental condition, that fluorescent MutL foci do not correspond to non-specific protein aggregates. Non-specific aggregates could be identified on the basis of their lifetime, which is expected to be longer than the lifetime of mutation-related foci. However, depending on the imaging conditions, photobleaching may limit the observed lifetime of the fluorescent foci. In addition, in some stressful conditions, the lifetime of the mutation-related foci may be more variable, particularly if replication is perturbed. Thus, to test for the presence of non-specific aggregates, a simple control procedure is to use a strain that expresses the MutL fluorescent protein and that is inactivated for the *mutS* gene. The MMR protein MutS is essential for MutL binding to DNA mismatches. If the fluorescent foci are caused by replication errors, they will disappear when *mutS* is inactivated. By contrast, foci created by non-specific protein aggregates will remain in the *mutS* background.

In the protocol described here for MV experiments, the fluorescent MutL is a fusion of MutL with YFP, although other fluorescent proteins could be used. In particular, other functional protein fusions have already been obtained, for instance, using mYPet, cyan fluorescent protein (CFP) or mCherry[13–15]. Likewise, visualization of the bacterial cells in both MV and μMA experiments can be performed by fluorescence imaging with any fluorophore that is homogeneously distributed in the cytoplasm, or by phase-contrast imaging. Our image analysis software BACMMAN can segment and track the cells from either fluorescence or phase-contrast images[12].

In the present protocol, we use the classic mother machine chip, as originally described in Wang et al.[11]. However, other types of mother machines could be used, such as the recently developed dual-input mother machine[16], which allows fine dynamical control of the growth conditions. For μMA, the geometry of the microchannels of the mother machine, that is, dead-end microchannels in which cells grow in single file, is essential to blocking natural selection. By contrast, for MV experiments, the geometry of the microchannels could be changed, for instance, to channels with two open ends or to larger chambers in which cells could grow in two dimensions, such as in the study by Dormeyer et al.[17], in which tandem repeat mutagenesis was investigated. However, in this case, using our image

analysis software BACMMAN would require the implementation of new plugins. As explained in the corresponding protocol[12], BACMMAN has a modular structure, which allows easy implementation of new plugins. This nevertheless requires a certain level of programming expertise.

MV and μMA protocols should be applicable to other *E. coli* strains. Furthermore, the μMA protocol can also be easily adapted for use with other rod-shaped microorganisms, such as *Bacillus subtilis* or *Saccharomyces pombe*, which can be cultivated in mother machine chips[18,19]. By contrast, because of the differences in MMR systems in different bacteria, it may be more challenging to adapt MV experiments to different bacterial species.

Note that MV and μMA can be combined in a single experiment, allowing the occurrences of fluorescent MutL foci and the fitness evolution during MA to be followed simultaneously. However, owing to mutation segregation and to potential delays between DNA modifications and phenotypic changes, establishing a one-to-one relationship between mutations and fitness changes is not currently possible, as explained in Robert et al.[1].

Current limitations

Fluorescent MutL foci allow the detection of mutations that are due to spontaneous DNA replication errors. This detection is very efficient, because MMR repairs 99% of replication errors. By contrast, we recently showed that fluorescent MutL foci do not allow the detection of mutations arising from the incorporation of 8-oxoguanine, an important source of mutations in normally growing cells[20]. Mutations originating from other chemically altered bases might be poorly detected by MutL as well. As shown in recent work by Uphoff[13], some replication errors that are due to DNA alkylation can be detected; however, the efficiency of this detection is unknown. Therefore, our detection method allows quantitative measurements of intrinsic DNA replication errors, but application of this method to the detection of mutations induced by DNA damage may not be quantitative. In this case, MutL foci may still be used as a proxy for mutagenic potential, as in Uphoff[13].

Several studies showed that the MMR proteins MutS and MutL can become limiting in some conditions, for instance, during treatments with certain antibiotics or with mutagens, during starvation or for mutant strains with a particularly high rate of replication error production[21–26]. In these conditions, in which the efficiency of MMR is decreased, mutations cannot be quantitatively estimated with our method.

Finally, our mutation detection method is limited by optical resolution. In particular, two spots cannot be separated if they are closer than ~200 nm. Consequently, mutations cannot be quantified for extremely high mutation rates (>500-fold increase in mutation rate compared to that of wild-type *E. coli*), which lead to numerous foci inside the cells (an *E. coli* cell of normal size in LB medium should not contain >4–5 foci). Likewise, our method would not allow detection of bursts of mutation if these are very local on the DNA (typically <80 kb). Given the speed of the polymerase (~1,000 nt/s), we estimate that our method would typically be blind to mutation bursts that last <1–2 min. However, such very transient bursts can be detected with our method if the mutation rate increases in the whole cell, for example, due to metabolic fluctuations or stochastic gene expression, as several replication forks are simultaneously active in the cell at different locations. Therefore, our method can detect very rapid bursts except if they occur at a single replication fork (such as could be created by a single aberrant polymerase protein).

Experimental design

Setting up an MV or μMA experiment requires multiple steps that we present in detail in this protocol. Before commencing the procedure, bacterial strains expressing a fluorescent MutL protein for mutation detection should be constructed or obtained from the authors upon request. Next, a mold for soft lithography with the design of the mother machine has to be bought or fabricated. Fabricating the mold requires microfabrication expertise, access to a clean room and costly chemicals. Therefore, for laboratories that are not usually engaged in a microfabrication activity, our advice is to outsource the fabrication of the mold, which can be faster and cost-effective. Several companies or facilities can provide this type of product, such as the Kavli Nanolab Delft (The Netherlands), Sigatec (Switzerland), Micro Resist Technology (Germany), Innopsys (France) and Cornell NanoScale Science and Technology Facility (USA). However, for those who wish to fabricate the mold themselves, examples of microfabrication protocols can be found in the supplementary information of Robert et al.[1] or in Taheri-Araghi and Jun[27]. Standard soft lithography is then required to obtain transparent polydimethylsiloxane (PDMS) microfluidic chips compatible with cell imaging. PDMS is first poured

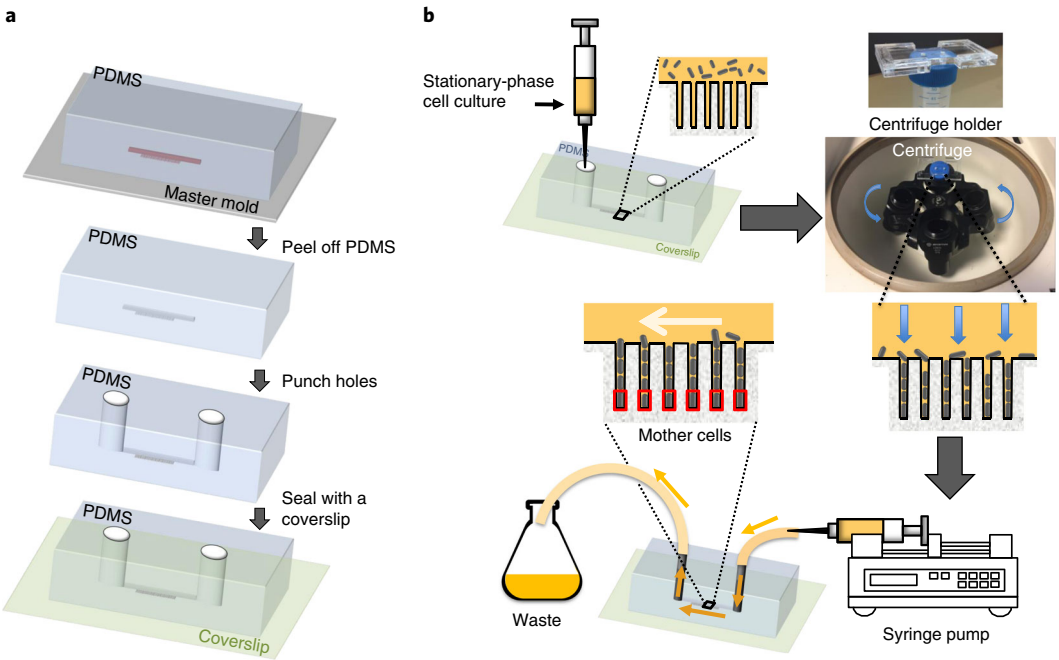

Fig. 3 | Fabrication and use of the mother machine microfluidic chip. a, Soft lithography. The PDMS chip is molded on a master mold, such as a silicon wafer with photoresist structures for the mother machine, then peeled off; holes are punched, and the device is sealed with plasma treatment. **b**, The cells are loaded into the device, pushed inside the microchannels by centrifugation, and the chip is connected to the syringe, which is installed on a syringe pump to deliver the flow of medium. The two pictures show our in-house-built centrifuge holder, which can accommodate one 24 × 60-mm coverslip with a mother machine chip sealed to it.

on the top of the mother machine mold, then baked, peeled away from the mold and bound to a glass surface by plasma treatment (Fig. 3a). Here, we describe the corresponding procedure in detail, but this part of the procedure is not specific to our method and other similar protocols for soft lithography can be applied (see, for instance, ref. [27]). Once the equipment is set up, bacteria are loaded into the growth microchannels, growth medium is flowed into the device (Fig. 3b), the device is mounted on the microscope and automated image acquisition is set. The last part of the procedure entails image processing using our custom-made software BACMMAN[12] and data analysis. Below, we describe considerations for each part of the process that should be addressed before commencing the procedure in greater detail.

Choice of the bacterial strains and culture conditions

Two critical parameters have to be taken into account. First, the width of the cells, which depends on the strain and the growth conditions, has to match the width of the microchannels. If the cell width is too large, the cells may not enter the microchannels or they may suffer mechanical stress during growth. By contrast, if cell width is too small, cells may overlap and pile up, wobble or swim inside the channels, preventing good imaging. Cell motility is also a critical parameter that depends on bacterial strain and growth conditions. Motility should be moderate, in order to prevent the cells from swimming outside the microchannels during the experiments. For example, the motility of some MG1655 strains may be too high, because of the presence of an insertion sequence in the regulatory region of the *flhD* gene. This is the case for the MG1655 strain that can be obtained from the *E. coli* Genetic Stock Center (CGSC 7740). We constructed our strains used in Robert et al.[1] from a poorly motile version of the strain MG1655, which can be found in the *E. coli* Genetic Stock Center (CGSC 6300). Non-motile mutants can also be used. It is possible that some sticking problems may occur with strains that are more susceptible to the formation of biofilms. However, we faced no particular problems when using an MG1655 strain carrying the F plasmid, known to increase biofilm formation[28].

Choice of microfluidic chip

We use the mother machine originally described in Wang et al.[11]. The dimensions of the microchannels have to be adapted to the strains and growth conditions used. Microchannel length should not exceed ~30 μm, to allow fast diffusion of nutrients along the microchannels and limit the

mechanical pressure exerted on the mother cell. If the experiments involve changing the growth conditions during time-lapse observation, we advise using the dual-input version of the mother machine[16]. As explained above, the geometry of the microchannels can be changed for MV experiments, but dead-end microchannels are required for μMA experiments.

Choice of imaging conditions

In both μMA and MV experiments, cells can be imaged by phase-contrast or fluorescence microscopy. For the image analysis stage, cell segmentation is usually easier using fluorescence images. However, with good imaging conditions (depending in particular on the optics of the microscope), BACMMAN performs almost as well at segmenting cells in phase–contrast images. In this case, phase contrast may be preferred to allow faster image acquisition and minimization of light exposure. The precision of growth rate estimation in μMA will depend on the number of images per cell cycle. We advise that at least four to five images per cell cycle be taken on average. For fluorescent spot imaging in MV experiments, the frequency of image acquisition should be sufficient to detect all mutations, that is, all long-lived MutL foci. Therefore, at least one to two images per cell cycle are required. In addition, to have a precise quantitative characterization of mutation dynamics, the acquisition frequency should be large compared to the mutation rate, so that the time interval between two successive mutations can be estimated with sufficient precision. The optimum exposure time and fluorescence intensity results from a trade-off between light toxicity and signal optimization. We advise doing preliminary experiments varying these parameters and measuring growth rate and average mutation rate, in order to find conditions at which the efficiency of mutation detection is satisfactory, but the growth rate is not impaired.

Control experiments

When doing MV experiments in conditions other than those reported in Robert et al.[1], we strongly advise checking that fluorescent MutL spots are not due to non-specific protein aggregation by using a *mutS* strain, as explained above. In some conditions, it may also be necessary to check that the natural level of MutS is sufficient to ensure efficient mutation detection. To do this, mutation rate should be estimated with natural expression or slight overexpression of MutS (strong overexpression may be toxic). In addition, we advise checking that the average lifetime of the long-lived foci that tag nascent mutations is as expected and equal to the doubling time. In our MV protocol, we use a strain in which the expression of YFP-MutL is under the control of the Plac promoter and therefore inducible with isopropyl β-D-1-thiogalactopyranoside (IPTG). Depending on the growth conditions, the leakiness of the promoter may allow detection of mutations without IPTG induction, or induction may be required. Therefore, the level of expression should be optimized before doing MV experiments. As fluorescent MutL is used both for error repair and for mutation detection, its expression level should (i) be sufficient to restore a wild-type mutation rate to the strain with a deletion of the native (non-fluorescent) *mutL*, which can be tested using classic fluctuation tests; and (ii) allow efficient mutation detection. If expression is too weak, it could limit the number of fluorescent MutL proteins that can accumulate in a spot, thus decreasing its fluorescence and making it harder to detect. By contrast, if the expression is too high, the cytoplasmic fluorescence due to unbound MutL will be too strong and foci detection will be harder. Note that the native MutL promoter can also be used instead of Plac. However, in that case, the fluorescence of the foci is less intense. For μMA experiments, before performing experiments with mutants, experiments should be performed with a wild-type strain to control for the stability of the setup on long time scales and to estimate the mutation-independent mortality rate.

Materials

Biological materials

- *For MV experiments. E. coli* MG1655 (CGSC 6300), with the native *mutL* and *lacZ* genes deleted, and expressing YFP-MutL and tdCherry proteins from the chromosome, *yfp-mutL* from the Plac promoter and *tdCherry* from the PRNA1 promoter. *yfp-mutL* is cloned in the *lacZ* chromosomal position and *tdCherry* between two Tn7 insertion sites. Details of the construction of this strain can be found in Robert et al.[1] ▲**CRITICAL** The deletion of the native *mutL* gene prevents the recruitment of non-fluorescent MutL proteins to the sites of DNA replication errors, which would decrease the fluorescence signal for mutation detection ▲**CRITICAL** The *yfp-mutL* fusion that we designed and constructed can be transferred into another *E. coli* strain by classic P1 transduction because we inserted a chloramphenicol (*cam*) resistance gene cassette downstream of *yfp-mutL*. Because the cloning of the *yfp-mutL-cam* fragment on the *E. coli* chromosome leads to *lacZ* gene deletion, blue–white screening can be used to identify positive clones among selected chloramphenicol-resistant bacteria. The DNA coding for the *yfp-mutL-cam* can also be amplified by PCR using our strain as a template or

synthesized de novo and inserted into another position on the *E. coli* chromosome using the Datsenko and Wanner gene replacement method[29] ▲ **CRITICAL** Do not use an *E. coli* strain with high motility.
- *For MV experiments.* *E. coli* MG1655 (CGSC 6300) expressing YFP-MutL and with the native chromosomal *mutL* and *mutS* genes deleted ▲ **CRITICAL** The presence of fluorescent foci in this strain indicates that the culture conditions lead to non-specific fluorescent MutL aggregates. Our method is not applicable in these conditions.
- *For μMA studies.* Any *E. coli* MG1655 (CGSC 6300) strain

Reagents

- LB broth (LB medium; Sigma-Aldrich, cat. no. L3022-1kg), supplemented if necessary with IPTG ▲ **CRITICAL** Although we used LB medium, other growth media can be used. Expression from the Plac promoter varies considerably depending on the growth medium. Therefore, the level of induction by IPTG should be optimized depending on the growth medium.
- Agar (Sigma-Aldrich, cat. no. A1296-1kg)
- IPTG (VWR, cat. no. 0487-10g)
- L-Arabinose (Sigma-Aldrich, cat. no. A3256-100g)
- Rifampicin (VWR, cat. no. 557303-5g)
- RTV615A + RTV615B (Eleco-Panacol, cat. no. RTV615) ! **CAUTION** RTV615 is a health grade level 1 compound with a flammability level of 1 and reactivity level of 0. Avoid inhalation and contact with skin, eyes, acids, bases and oxidizing substances.
- BSA (Sigma-Aldrich, cat. no. A4503-10g)
- Isopropanol (VWR, cat. no. 20842.298 1L) ! **CAUTION** Isopropanol is a health grade level 1 compound with a flammability level of 3 and reactivity level of 0. Store in a cool, dry, well-ventilated area. Keep away from all possible ignition sources. Avoid contact with eyes and skin.
- Ethanol (VWR, cat. no. 20821.296 1L) ! **CAUTION** Ethanol is a health grade level 2 compound with a flammability level of 3 and reactivity level of 0. Store in a cool, dry, well-ventilated area. Keep away from all possible ignition sources. Avoid contact with eyes and skin.
- Methanol (Sigma-Aldrich, cat. no. 179957-1L) ! **CAUTION** Methanol is a health hazard level 1 compound with a flammability level of 3 and an instability/reactivity level of 0. Avoid contact with skin and eyes, and avoid inhalation. Store and use in a well-ventilated area.
- Milli-Q filtered water

Equipment

▲ **CRITICAL** These are the specifications for the equipment that we use for performing MV and μMA experiments. Note that any equivalent equipment can be used for each.
- Laminar flow hood (ADS Laminaire, model nos. MSC-II-48 and Optimale 18)
- Master mold ▲ **CRITICAL** The initial design comprises thousands of identical rectangles. The specific dimensions must be optimized for particular applications and are dependent also on the fabrication technique.
- Tubes (polypropylene; 1.5, 15 and 50 ml; Fisher Scientific, cat. nos. 02-682-002, 14-959-49B and 14-959-49A, respectively)
- Petri dishes (VWR, cat. no. 663102)
- Incubator shaker (Infors HT, Ecotron model)
- Tabletop centrifuge (Eppendorf, MiniSpin model)
- Vortex (Heidolph, model no. REAX 2000)
- Vacuum bell jar
- Incubators (Memmert, model no. 300)
- Punch (0.75 mm; World Precision Instruments, cat. no. 504529)
- Plasma cleaner (Harrick Plasma, model no. PDC-002)
- Glass microscope slides (76 mm × 26 mm; Knittel Glass, cat. no. VA111001FKB.01)
- Glass microscope coverslips (24 mm × 60 mm; Knittel Glass, cat. no. VD12460Y1A.01)
- Scalpel blades (Swann-Morton, cat. no. 0503)
- Syringes (1 and 50 ml; VWR, cat. nos. SS+01T1 and SS+50ES1)
- Syringes (150 ml; Covidien, cat. no. 8881114063)
- Syringe filters (0.2 μm; Sartorius, cat. no. 16534-K)
- Luer stubs (blunt needles) (23 gauge × 0.5 inches; Phymep, cat. no. LS23)
- Tygon ND-100-80 (i.d. 0.02 inches, o.d. 0.06 inches; Phymep, cat. no. AAD04103)

- Vacuum filtration system (0.2 µm; Thermo Fisher Scientific, cat. no. 568-0020)
- Stainless-steel catheter couplers (23gauge × 8 mm; Phymep, cat. no. SC23/8)
- Holder for the microfluidic device on the microscope stage ▲CRITICAL The holder should allow complete immobility of the device relative to the microscope stage. Therefore, the holder should hold the coverslip tightly and there should be no mechanical slack of the holder on the stage.
- Vacuum pumps (Vacuubrand, Diaphragm Vacuum Pump MD1 model)
- Erlenmeyer flasks
- Oxygen bottle (Oxygene Smartop; Alphagaz)
- Metal spatula
- Syringe pumps (KD Scientific, model no. KDS Legato 270 for syringes of up to 60-ml volume; Harvard Apparatus, model PHD Ultra for syringes of up to 140-ml volume)
- Epi-fluorescence microscope equipped with a temperature-controlled chamber, an ×100 oil-immersion objective with high numerical aperture (NA 1.4), an automated stage, an infrared-based system for focus drift correction, fluorescence filters, light source, and EMCCD or sCMOS camera. We used two different microscopy setups for fluorescence imaging (MV experiment) and for phase-contrast imaging (µMA experiment). For the MV experiments, we used an inverted DeltaVision Elite microscope equipped with the Ultimate Focus system, an ×100 oil-immersion objective (NA 1.4), the DV Light Solid State Illuminator 7 Colors, a temperature-controlled chamber and the DV Elite sCMOS Camera. For the µMA experiments, we used an inverted Nikon Eclipse Ti-E microscope equipped with the Perfect Focus system, an external phase unit, a Uniblitz VMM-D1 shutter, a Plan APO ×100 oil-immersion objective (NA 1.4), a temperature-controlled chamber, a 100-W halogen lamp and a Hamamatsu CCD C8484-05G camera. However, any parts of these two systems, as well as any equivalent commercially available system, can be used for both MV and µMA experiments.
- Aluminum foil
- Scalpels
- Adhesive tape (Scotch)
- Binocular loupe
- Paper towels
- Eppendorf tubes

Software

- BACMMAN[12] (for installation of the software, see https://github.com/jeanollion/bacmman/wiki) ▲CRITICAL To allow fast and reliable analysis of MV and µMA datasets, we recently developed BACMMAN, a Java-based software compatible with Linux, Windows and Mac OS and easily installed through Fiji. It allows detection, segmentation and tracking of bacteria and intracellular fluorescent spots, enables easy visualization and manual editing of the results and has a user-friendly graphical user interface. We describe BACMMAN and give a precise protocol to install and run it in Ollion et al.[12]. Furthermore, to help the user discover the software and all its functionalities, we also provide two small datasets from typical MV and µMA experiments[12].
- Fiji (https://imagej.net/Fiji/Downloads)

Reagent setup

BSA stock solution (10 mg/ml)

Dissolve BSA in Milli-Q water. After the BSA has dissolved completely (avoid mixing vigorously), filter with 0.2-µm filters. Make 1-ml aliquots. BSA stock solution can be prepared in advance and stored at −20 °C for up to a year. Upon defrosting, the solution should be kept on ice. Avoid re-freezing leftovers.

LB medium

LB medium should be prepared and stored according to the manufacturer's instructions.

Rifampicin

Antibiotic solutions should be prepared and stored according to the manufacturer's instructions.

IPTG solution (1 M)

Dissolve IPTG in Milli-Q water. After the IPTG has dissolved completely, filter with 0.2-µm filters. Make 1-ml aliquots. IPTG stock solution can be prepared in advance and stored at −20 °C for up to a year. Upon defrosting, the solution should be kept on ice.

Procedure

Preparing the cells ● Timing 10 min + overnight incubation

1 Starting from a glycerol stock, grow an overnight culture of the desired strain in LB medium at 37 °C. Add IPTG to the growth medium when necessary ('Experimental design' section).

2 In the morning, check that the overnight culture is saturated and transfer 1 ml of the overnight culture to a sterile Eppendorf tube (1.5 ml). Concentrate the cells by centrifuging at 12,000*g* for 1 min (20 °C), discarding 900 µl of the supernatant and resuspending the pellet in the remaining 100 µl of the supernatant. Leave at room temperature (RT; 20 °C).
▲ **CRITICAL STEP** Because cell density varies for different growth media, this step needs to be optimized for each growth condition.

Fabricating the PDMS microfluidic chip ● Timing 2 h + baking overnight

3 Mix RTV615A and RTV615B in a 10:1 ratio in a clean 50-ml polypropylene tube. The prepared amount should be sufficient to cover the master mold entirely, with a thickness of ~5 mm. Mix vigorously for 1–2 min with a metal spatula.
! **CAUTION** RTV615B is less viscous than RTV615A. Proceed slowly while adding it to the RTV615A. Use gloves for handling RTV615A and RTV615B, as these compounds are sticky, and use aluminum foil to protect all equipment from contact with RTV615 compounds.
▲ **CRITICAL STEP** For fabricating the PDMS chips, we use RTV615 silicone rubber compounds from Momentive. RTV615A is a clear liquid and cures to silicone rubber after the addition of the curing agent, RTV615B.

4 Degas the mix by centrifuging at 3,400*g* for 1 min (20 °C).

5 Place the master mold on a flat surface. Pour the mix on the top of the master mold to cover the whole surface evenly with a thickness of ~5 mm.
▲ **CRITICAL STEP** Proceed slowly to avoid making air bubbles.
▲ **CRITICAL STEP** If the master mold is on a silicon wafer, it should be stuck to the bottom of a Petri dish before pouring the PDMS.
▲ **CRITICAL STEP** To ensure optimal connection of the microfluidic chip with the tubing, the thickness of the PDMS should not be <4 or >7 mm.

6 Put the mold with freshly poured PDMS in a vacuum bell jar, apply vacuum for 1 min, then turn the vacuum off and leave the chip in the vacuum bell jar for 5 min. Air bubbles will form in the PDMS and move to its surface. To burst the bubbles, disrupt the vacuum by bringing air into the jar briefly. Repeat this step twice.

7 Take the mold out of the vacuum bell jar and leave it on a flat surface at RT for 1 h to ensure full elimination of air bubbles.
▲ **CRITICAL STEP** Degassing is important, because air bubbles trapped in the PDMS can prevent the molding of the microchannels and/or change the light-scattering properties of the material, thus degrading the imaging conditions. Do not apply vacuum for >1 min or PDMS will foam out of the mold.
▲ **CRITICAL STEP** Do not wait too long before proceeding to bake the chip; otherwise, the PDMS will cure at RT, which changes its consistency.

8 Bake overnight at 65 °C.
▲ **CRITICAL STEP** You should place the mold with PDMS on a flat surface to avoid producing a chip with a tilted surface

9 Remove the mold with the cured PDMS from the oven.

10 Leave the mold at RT for a few minutes so that it cools.
■ **PAUSE POINT** Cured PDMS can be left on the mold for several days. Older PDMS chips can also be used, but the properties of the PDMS material might be slightly altered.

11 After cooling, use a clean scalpel to cut the chip from the cured PDMS. The chip dimensions should be compatible with those of the glass slide and the device holder on the microscope stage. Peel the chip from the mold gently.
! **CAUTION** Avoid cutting the PDMS too close to the structure containing the required features and take care not to touch the features with the scalpel or with your fingers. Do not press strongly while cutting to avoid personal injury and to avoid breaking the mold, in particular when using silicon wafers, which can easily break. Likewise, peeling of PDMS should be done gently to avoid damaging the mold.
? **TROUBLESHOOTING**
■ **PAUSE POINT** The PDMS chips can be stored at RT protected from dust for several days. If necessary, dust can be removed by applying adhesive tape.

12 To create the inlet and outlet of the device, punch a hole at both ends of the main trench using a 0.75-mm World Precision Instruments punch. To do this, put the PDMS chip on a glass slide. The side of the chip where the channels are printed should be positioned upward. To precisely locate the main trench ends, where the holes should be punched, punching can be performed under a binocular loupe. Bring the punch to the appropriate locations and gently push it through the PDMS.
▲ **CRITICAL STEP** The punch should be clean. Change the punch frequently, before it becomes blunt; otherwise, it may produce PDMS fragments that could clog the device.
▲ **CRITICAL STEP** Check that the two holes are properly located at each end of the main trench. Make sure that the small pieces of the punched PDMS came out of the holes.

13 Clean the PDMS surfaces with adhesive tape to remove small PDMS pieces and dust.
▲ **CRITICAL STEP** We recommend performing Steps 13–18 under a hood to protect the surfaces from dust.

14 Clean a glass microscope coverslip with isopropanol to remove dirt and dust and dry it with a clean dry air jet.

15 Place the cleaned PDMS device with its features upward and the coverslip in the plasma cleaner machine. Oxygen plasma will modify the surface of the PDMS and the glass so that they can be sealed together irreversibly. This allows closure of the PDMS device with the coverslip.
▲ **CRITICAL STEP** Make sure you apply the plasma treatment to the appropriate side of the PDMS chip by placing the side with the channels upward in the plasma cleaner.

16 Perform an oxygen plasma treatment according to your machine's protocol.
▲ **CRITICAL STEP** Inject the oxygen slowly. Otherwise, the coverslip and PDMS chip might be blown away and turn upside down inside the plasma cleaner.

17 Break the vacuum, open the plasma cleaner and take the chip and the coverslip out.

18 Put the two surfaces (the plasma-treated sides) in contact rapidly without applying pressure by gently laying the PDMS device on the glass.
▲ **CRITICAL STEP** In the case that air pockets form, gently tap the device to ensure complete contact.
▲ **CRITICAL STEP** Lay the PDMS chip in the middle of the coverslip with the main channel parallel to the coverslip edges to facilitate image acquisition.

19 Incubate the assembled PDMS device at 80 °C for 10 min. This step enhances bonding.

20 Remove the device from the oven and leave it on the bench (at RT) for a few minutes until it cools.
? TROUBLESHOOTING

21 Using a 1-ml syringe, take up ~100 µl of 10 mg/ml BSA. Surface treatment with BSA prevents cell adhesion. Connect a blunt needle (Luer stub) to the syringe. Then insert the needle into one of the holes you previously drilled in the PDMS. Gently push the plunger of the syringe. A couple of seconds later, the BSA solution will come out from the other hole. Place a small piece of paper towel in a Petri dish and put the device on it. Place another small piece of paper towel soaked in water in the Petri dish and close the dish. Leave at RT for 2 h.
▲ **CRITICAL STEP** The soaked paper towel avoids evaporation of the BSA solution in the device. Once sealed, the device should always be filled with liquid; otherwise, it will lose the hydrophilicity created by the plasma treatment.
▲ **CRITICAL STEP** When injecting the BSA solution, check that the device does not leak.
■ **PAUSE POINT** The chip filled with BSA can be stored overnight at 4 °C.

Loading the cells into the device ● Timing 20 min

22 Briefly vortex the 10× concentrated overnight cell culture obtained in Step 2. Then take it up with a 1-ml syringe with a blunt needle. Insert the needle into one of the device holes and gently push the plunger of the syringe. A couple of seconds later, the cell suspension will come out from the other hole. Carefully remove the needle.

23 Seal the inlet and outlet with adhesive tape.

24 Place the device in a centrifuge and spin at 520*g* for several minutes (20 °C). The device should be installed in the centrifuge such that the centrifugal force will push the cells floating in the main channel into the microchannels. Remove the device and check the loading of the cells into the microchannels under a microscope. Repeat this step if loading is insufficient.
▲ **CRITICAL STEP** A holder should be fabricated to hold the device in the centrifuge. The geometry of the holder should allow the centrifugal force to push the cells into the microchannels. An example of a suitable holder is shown in Fig. 3.

▲ CRITICAL STEP The loading efficiency depends on the size of the cells and the width and height of the microchannels. Because cells tend to be smaller when grown in poorer media, cultivating cells in a poor growth medium before injection into the device can increase the loading efficiency.

▲ CRITICAL STEP Ensure that the device and the cells do not dry out. Deliver fresh growth medium as soon as the cells are loaded into the device.

? TROUBLESHOOTING

Preparing the growth medium ● Timing 25 min

25 Add BSA to the desired amount of LB medium in order to obtain 0.1 mg/ml BSA. Add IPTG for induction of fluorescent MutL expression if necessary (full induction of the Plac promoter can be obtained with 1 mM IPTG).

▲ CRITICAL STEP BSA is necessary to prevent the cells from sticking to the surfaces in the main channel.

26 Filter the medium with a vacuum filtering system and dispense it into a syringe of the appropriate volume.

▲ CRITICAL STEP The amount of prepared medium depends on the time scale of the experiment. During the experiment, the typical flow rate is 2 ml/h.

27 Prepare the inlet and outlet tubing by cutting two pieces of Tygon tubing with i.d. 0.02 inches and o.d. 0.06 inches.

▲ CRITICAL STEP The length of the inlet tubing will depend on the distance between the syringe pump and the device once it is set on the microscope. Check this distance before starting the experiment and cut a piece of tubing of appropriate size. Likewise, the length of the outlet tubing will depend on the distance between the device and the flask that will collect the medium flowing outside the outlet tubing.

28 Insert a blunt needle into one end of the inlet tubing and a stainless-steel catheter coupler into the other end.

29 Insert a clean stainless-steel catheter coupler into one end of the outlet tubing.

▲ CRITICAL Wear gloves and work under a laminar hood to avoid contamination. Clean the couplers and needles with ethanol and dry them before inserting them into the tubings.

30 Get rid of any air bubbles trapped in the syringe containing the growth medium. To do so, gently tap the syringe barrel to detach the bubbles from the walls and let them go up to the tip of the syringe.

31 Connect the syringe to the needle of the inlet tubing. Push slightly on the plunger to completely fill the inlet tubing with medium.

Flowing the medium into the device ● Timing 15 min

32 Place the end of the inlet tubing into an Erlenmeyer flask or a similar receptacle. Place the syringe with the inlet tubing on the syringe pump and start pumping the medium at high flow rate (e.g., 30 ml/h) until ~1 ml of medium flows out of the tubing. This will ensure that the pusher block is completely pushed against the syringe plunger. Then decrease the flow rate to 5 ml/h.

33 Remove the adhesive tape from the PDMS of the microfluidic device. Insert the coupler at the end of the outlet tubing into one of the two holes of the device and place the other end of the outlet tubing into a flask that will collect the used medium during the experiment. Then insert the coupler at the end of the inlet tubing into the other hole of the device.

▲ CRITICAL STEP Make sure the stainless-steel catheter couplers are inserted properly and deeply enough. They should almost touch the coverslip.

▲ CRITICAL STEP Connection of the inlet tubing to the device should be performed without stopping the flow, so that the bacteria cannot swim inside the inlet tubing. Likewise, avoid moving the device up and down once it is connected to the inlet tubing, to avoid creating a flow from the chip to the inlet tubing that may bring bacteria inside the inlet tubing. The diameter of the inlet tubing is much larger than the width of the chip's main channel, so the flow may not be sufficient to remove all the bacteria from the inlet tubing once it is contaminated. For long time scale experiments, contamination of the inlet tubing leads to the formation of a biofilm, which can change the composition of the medium diffusing into the microchannels and flush out many cells that can stick in the main channel. When contamination of the inlet tubing is observed, the experiment should be stopped and the data should be discarded.

▲ CRITICAL STEP Use gloves to avoid contamination.

34 When the liquid begins flowing out of the chip in the outlet tubing, decrease the flow rate to 2 ml/h.

▲ CRITICAL STEP Take care not to increase the flow rate to >100 ml/h for more than a couple of minutes because such a high flow rate may damage the device and cause leaks. A 5-ml/h flow rate should be sufficient to flush away all the cells from the main trench. As a result, only the cells loaded

in the growth microchannels will remain inside the device. Sometimes, a higher flow rate of 10–40 ml/h might be necessary to clean the main trench of PDMS fragments.
? TROUBLESHOOTING

Automatic image acquisition ● Timing 3 h

35 Mount the device on your microscope.
▲ CRITICAL STEP Avoid moving the device up and down more than necessary, to avoid creating a flow from the chip to the inlet tubing.
▲ CRITICAL STEP Before placing the device, the microscope needs to be switched on and set up for image acquisition. Temperature variations should be avoided during the experiment. Therefore, the microscope chamber should be set to 37 °C several hours before beginning the experiment, and all the components of the system susceptible to producing heat should also be switched on in advance. As an example, the Perfect Focus system of the Nikon Eclipse microscope should be turned on several hours before beginning the experiment.

36 Check that there are no leaks in the device and leave it on the microscope for 2 h 30 min.

37 Configure the time-lapse experiment on the acquisition software and launch the acquisition.
▲ CRITICAL STEP Users need to determine the optimal time-lapse configuration for their system and purposes (e.g., excitation light intensity and exposure time, number of fields of view and number of time steps), as explained in the 'Experimental design' section. For our equipment and conditions, we use the following setup. We record images at ×100 magnification in phase contrast every 4 min for μMA experiments and in fluorescence every 2 min for MV experiments. For MV experiments, we use excitation light at 575 nm (tdCherry excitation) and 513 nm (YFP excitation), 0.1-s exposure with illumination intensity set to 3.5% of the maximum LED intensity for tdCherry, and 2-s exposure at 7.5% of the maximum LED intensity for YFP.
▲ CRITICAL STEP Check regularly for device leaks during image acquisition.
? TROUBLESHOOTING

Troubleshooting

Troubleshooting advice can be found in Table 1.

Table 1 | Troubleshooting table

Step	Problem	Possible reason	Solution
11	Peeled PDMS is too soft	PDMS may have partially cured at RT before baking	Decrease the time delay before baking
20	The PDMS does not bind strongly to the coverslip	Plasma treatment was not performed optimally	Clean the plasma cleaner chamber, optimize the parameters (e.g., oxygen pressure and plasma exposure time), try longer incubation time at 80 °C after plasma treatement
24	Many microchannels are not filled with cells	The cell concentration is too low or too high in the main channel or cells aggregate	Adjust the cell concentration and vortex to break aggregates
		Cells are too large to enter the microchannels	Grow cells in poorer medium to decrease their diameter or use another mold
34	The growth medium is not passing through the device	PDMS debris is clogging the main trench	Momentarily increase the flow rate
	The device is leaking	Sealing was not done correctly	Use another microfluidic device
37	Cells swim outside the growth channels	Motility is too high	Use a poorly motile or non-motile strain
	Cells stick to the PDMS and/or glass	BSA is too old or the concentration is too low	Use the appropriate concentration of fresh BSA
		Plasma treatment did not work properly	Check the parameters of the plasma treatment
	Cells have weird shapes	The genetic background of the strain is not appropriate	Use the strain MG1655 6300
	Yellow fluorescence is too low	IPTG was omitted from the growth medium	Add IPTG to the growth medium
	The quality of the images decreases during the experiment	Focus was lost	Switch on all the components of the microscopy setup (including the focus drift correction system) several hours before putting the device on the microscope

Timing

All approximate timings are for a typical MV or μMA experiment.
Steps 1 and 2, preparing the cells: 10 min + overnight incubation
Steps 3–21, fabricating the PDMS microfluidic chip: 2 h + baking overnight
Steps 22–24, loading the cells into the device: 20 min
Steps 25–31, preparing the growth medium: 25 min
Steps 32–34, flowing the medium into the device: 15 min
Steps 35–37, automatic image acquisition: 3 h

Anticipated results

MV experiments

MV experiments allow a precise quantitative characterization of the dynamics of point mutations created by replication errors in *E. coli*. In particular, they allows investigation of single-cell variability in the rate of occurrence of these mutations. As mutations are detected in single cells, it is also possible to correlate the frequency of their occurrence with single-cell phenotypes such as growth rate, cell morphology or the expression of specific markers[1,15]. We discuss here how to analyze and interpret the data from MV experiments.

Characterization of the mutagenesis process

Although mutations can be detected in all the cells present in a microchannel, we advise analyzing only the mother cell, at least to begin with. In terms of data analysis, this allows the simple framework of time series, and therefore simple and powerful mathematical tools, to be used. Analyzing all cells in the microchannels requires much more complex mathematical tools adapted to the analysis of binary trees. Once the time series of mutation occurrences in mother cells for all the microchannels have been extracted from the images, the mutation occurrences can be characterized mathematically. To do so, a particularly relevant variable is the inter-arrival time, that is, the time between the occurrence of the mutation i and the mutation $i + 1$. Poissonian dynamics leads to exponentially distributed inter-arrival times. It is important to keep in mind that the inter-arrival times that we measure can take only discrete values that are multiples of the time step of image acquisition. Consequently, the distribution of measured inter-arrival times is slightly biased, the 0 value being underrepresented compared to the distribution of the 'real' inter-arrival times[1]. In the case of a Poisson process, the distribution of the measured inter-arrival times can be calculated exactly, as described in the supplementary methods of Robert et al.[1].

Single-cell analysis of the replication error rate requires the estimation of the error rate per replicated base

Visualization of replication errors in single cells allows the comparison of the error rates in different subpopulations of cells and correlation of the error rates with other phenotypes. Obtaining the error rate per cell, that is, the rate at which replication errors occur in a single cell is straightforward in the MV approach. However, differences in the per-cell error rate of different subpopulations of cells do not necessarily reflect differences in their DNA replication fidelity or DNA repair efficiency. This is because the number of MutL foci in a single cell depends not only on the cell's replication and repair proficiency but also on its number of active replication forks. In bacteria, several replication cycles can overlap; depending on the growth conditions and the stage in the cell cycle, the number of active replication forks in a single *E. coli* cell can vary from 0 to 12 (refs. [30,31]). Thus, the per-cell replication error rate of different subpopulations reflects not only their replication and repair proficiency but also their average cell cycle stage and growth rate.

For specifically accessing the differences in DNA replication and repair proficiency among different subpopulations, the error rate should be estimated per replicated base. This can be obtained by normalizing the number of MutL foci by the number of replication forks per cell, which requires knowledge of how many replication forks are present in the cells. Ideally, the number of replication forks can be visualized in MV experiments (simultaneously with MutL foci) by using a fluorescent marker of the replisome[32]. However, for *E. coli*, whose cell cycle has been deciphered in detail, it is possible to estimate the average number of replication forks from the growth rate of the cells and their size, a proxy for their cell cycle stage. Although the stochasticity of the cell cycle precludes the use of such a model to determine the number of forks precisely for each single cell, the average number of

forks can be estimated and used to normalize the rate of the occurrence of MutL foci in the different subpopulations of cells with different cell sizes and/or growth rates. If such analysis is not performed, some growth and cell cycle differences (for different subpopulations or different strains or in different growth conditions) may be misinterpreted as differences in replication and repair proficiency.

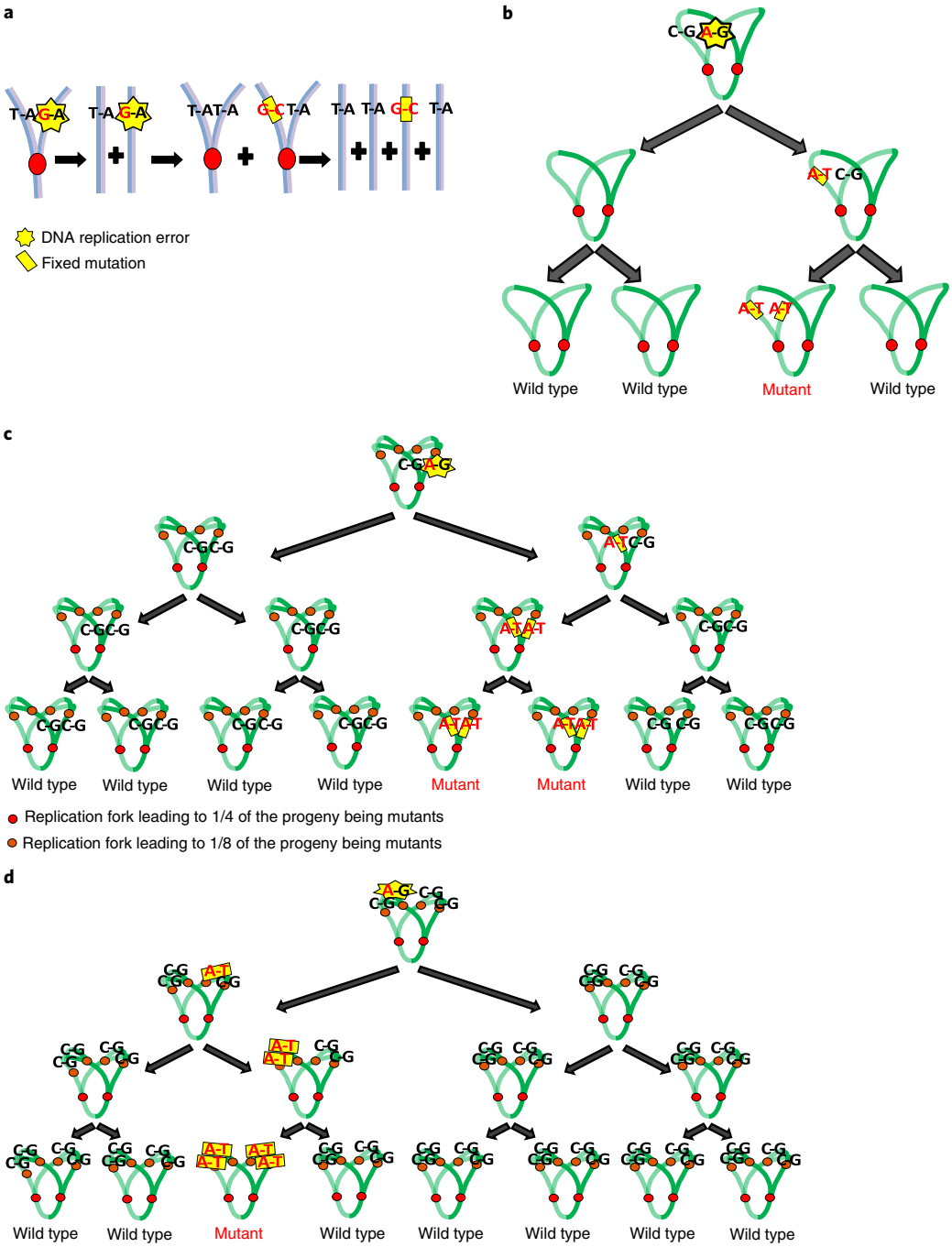

Fig. 4 | Replication errors and mutation fixation. a, An erroneous base (yellow star) incorporated during one round of replication (the replisome is represented as a red dot) is converted into a mutation during the next round of replication, leaving one mutated DNA molecule out of 4. **b**, When replication cycles do not overlap, that is, when the replication time is smaller than the doubling time, a replication error observed as a YFP-MutL spot in one cell leads to 1/4 of the cell's progeny being mutants. **c**,**d**, Examples of mutation fixation for multifork replication, that is, when the replication time is larger than the doubling time. **c**, The error is introduced by one of the replication forks shown in red, leading to 1/4 of the progeny being mutants. By contrast, the error is introduced by one of the replication forks shown in orange, leading to 1/8 of the progeny being mutants (**d**).

μMA experiments

μMA experiments have been designed to characterize the DFE of spontaneous mutations. Using a simple model described in Robert et al.[1], all the moments of the DFE, such as the mean, the variance or the skewness, can be easily estimated from the temporal evolution of the fitness distribution, that is, the distribution of single-cell growth rates. This is explained in detail in the supplementary methods of Robert et al.[1], where all the necessary formulas can be found. In Robert et al.[1], μMA experiments were used to investigate the effects of point mutations created by replication errors and we estimated the mutation rate independently, using MV experiments. This independent estimation is important for quantitative DFE estimation and is explained below.

Calculation of the mutation rate from the rate of occurrence of MutL foci

Long-lived MutL foci tag unrepaired DNA replication errors (mismatches), which give rise to mutations. In this section, we explain how the rate of occurrence of such foci can be used to calculate the rate of mutation fixation during a μMA experiment. When an error occurs during the replication of a double-stranded DNA molecule, the genetic information is altered on only one strand of one of the two double-stranded DNA molecules. Therefore, after another round of replication, only one of the four double-stranded DNA molecules will carry the mutation (Fig. 4a). Therefore, in *E. coli*—in conditions in which a single replication cycle is ongoing, such as in poor medium—when a MutL focus is observed in one cell, 1/4 of its progeny will be mutated (Fig. 4b). This proportion can be lower in the case of multifork replication, such as in rich medium, when the doubling time is shorter than the time necessary to replicate the chromosome. For instance, if the cell contains six replication forks, for two of them, an error will lead to a proportion of one-quarter of mutants in the progeny, whereas for the four other forks, an error will lead to a proportion of one-eighth of mutants in the progeny (Fig. 4c,d). For a given rate of growth, the average proportion p of mutant cells in the progeny of a cell containing a MutL focus can be calculated on the basis of classic models of the bacterial cell cycle. An example can be found in the supplementary methods of Robert et al.[1]. Once p has been calculated, the mutation rate m in the mother cell lines in μMA experiments can be obtained by multiplying the rate of the occurrence of long-lived MutL foci L by p: $m = L \times p$.

Reporting Summary

Further information on research design is available in the Nature Research Reporting Summary linked to this article.

Data availability

No datasets were generated or analyzed during the current study. Datasets from a related study are archived at Dryad (https://doi.org/10.5061/dryad.75625).

References

1. Robert, L. et al. Mutation dynamics and fitness effects followed in single cells. *Science* **359**, 1283–1286 (2018).
2. Luria, S. E. & Delbruck, M. Mutations of bacteria from virus sensitivity to virus resistance. *Genetics* **28**, 491–511 (1943).
3. Foster, P. L. Methods for determining spontaneous mutation rates. *Methods Enzymol.* **409**, 195–213 (2006).
4. Frenoy, A. & Bonhoeffer, S. Death and population dynamics affect mutation rate estimates and evolvability under stress in bacteria. *PLoS Biol.* **16**, e2005056 (2018).
5. Nishant, K. T., Singh, N. D. & Alani, E. Genomic mutation rates: what high-throughput methods can tell us. *Bioessays* **31**, 912–920 (2009).
6. Mukai, T. The genetic structure of natural populations of *Drosophila melanogaster*. I. Spontaneous mutation rate of polygenes controlling viability. *Genetics* **50**, 1–19 (1964).
7. Eyre-Walker, A. & Keightley, P. D. The distribution of fitness effects of new mutations. *Nat. Rev. Genet.* **8**, 610–618 (2007).
8. Halligan, D. L. & Keightley, P. D. Spontaneous mutation accumulation studies in evolutionary genetics. *Annu. Rev. Ecol. Evol. Syst.* **40**, 151–172 (2009).
9. Heilbron, K., Toll-Riera, M., Kojadinovic, M. & MacLean, R. C. Fitness is strongly influenced by rare mutations of large effect in a microbial mutation accumulation experiment. *Genetics* **197**, 981–990 (2014).
10. Elez, M. et al. Seeing mutations in living cells. *Curr. Biol.* **20**, 1432–1437 (2010).
11. Wang, P. et al. Robust growth of *Escherichia coli*. *Curr. Biol.* **20**, 1099–1103 (2010).

12. Ollion, J., Elez, M. & Robert, L. High-throughput detection and tracking of cells and intracellular spots in mother machine experiments. *Nat. Protoc.* https://doi.org/10.1038/s41596-019-0216-9 (2019).
13. Uphoff, S. Real-time dynamics of mutagenesis reveal the chronology of DNA repair and damage tolerance responses in single cells. *Proc. Natl. Acad. Sci. USA* **115**, E6516–E6525 (2018).
14. Elez, M., Radman, M. & Matic, I. Stoichiometry of MutS and MutL at unrepaired mismatches in vivo suggests a mechanism of repair. *Nucleic Acids Res.* **40**, 3929–3938 (2012).
15. Woo, A. C., Faure, L., Dapa, T. & Matic, I. Heterogeneity of spontaneous DNA replication errors in single isogenic *Escherichia coli* cells. *Sci. Adv.* **4**, eaat1608 (2018).
16. Kaiser, M. et al. Monitoring single-cell gene regulation under dynamically controllable conditions with integrated microfluidics and software. *Nat. Commun.* **9**, 212 (2018).
17. Dormeyer, M. et al. Visualization of tandem repeat mutagenesis in *Bacillus subtilis*. *DNA Repair* **63**, 10–15 (2018).
18. Norman, T. M., Lord, N. D., Paulsson, J. & Losick, R. Memory and modularity in cell-fate decision making. *Nature* **503**, 481–486 (2013).
19. Nakaoka, H. & Wakamoto, Y. Aging, mortality, and the fast growth trade-off of *Schizosaccharomyces pombe*. *PLoS Biol.* **15**, e2001109 (2017).
20. Foster, P. L., Lee, H., Popodi, E., Townes, J. P. & Tang, H. Determinants of spontaneous mutation in the bacterium *Escherichia coli* as revealed by whole-genome sequencing. *Proc. Natl. Acad. Sci. USA* **112**, E5990–E5999 (2015).
21. Schaaper, R. M. *Escherichia coli* mutator mutD5 is defective in the mutHLS pathway of DNA mismatch repair. *Genetics* **121**, 205–212 (1989).
22. Elez, M., Radman, M. & Matic, I. The frequency and structure of recombinant products is determined by the cellular level of MutL. *Proc. Natl. Acad. Sci. USA* **104**, 8935–8940 (2007).
23. Negishi, K., Loakes, D. & Schaaper, R. M. Saturation of DNA mismatch repair and error catastrophe by a base analogue in *Escherichia coli*. *Genetics* **161**, 1363–1371 (2002).
24. Gutierrez, A. et al. β-Lactam antibiotics promote bacterial mutagenesis via an RpoS-mediated reduction in replication fidelity. *Nat. Commun.* **4**, 1610 (2013).
25. Harris, R. S. et al. Mismatch repair protein MutL becomes limiting during stationary-phase mutation. *Genes Dev.* **11**, 2426–2437 (1997).
26. Maas, W. K., Wang, C., Lima, T., Hach, A. & Lim, D. Multicopy single-stranded DNA of *Escherichia coli* enhances mutation and recombination frequencies by titrating MutS protein. *Mol. Microbiol.* **19**, 505–509 (1996).
27. Taheri-Araghi, S. & Jun, S. in *Hydrocarbon and Lipid Microbiology Protocols: Single-Cell and Single-Molecule Methods* (eds McGenity, T. J. et al.) 5–16 (Springer, 2015).
28. Ghigo, J. M. Natural conjugative plasmids induce bacterial biofilm development. *Nature* **412**, 442–445 (2001).
29. Datsenko, K. A. & Wanner, B. L. One-step inactivation of chromosomal genes in *Escherichia coli* K-12 using PCR products. *Proc. Natl. Acad. Sci. USA* **97**, 6640–6645 (2000).
30. Cooper, S. & Helmstetter, C. E. Chromosome replication and the division cycle of *Escherichia coli* B/r. *J. Mol. Biol.* **31**, 519–540 (1968).
31. Zaritsky, A., Wang, P. & Vischer, N. O. Instructive simulation of the bacterial cell division cycle. *Microbiology* **157**, 1876–1885 (2011).
32. Reyes-Lamothe, R., Possoz, C., Danilova, O. & Sherratt, D. J. Independent positioning and action of *Escherichia coli* replisomes in live cells. *Cell* **133**, 90–102 (2008).

Acknowledgements

This work was funded by the Agence Nationale de Recherche (grant ANR-14-CE09-0015-01 to M.E.) and by the city of Paris (program Emergences 2018 to M.E.).

Author contributions

L.R. and M.E. developed the protocol. J.O. developed the image analysis software. L.R., M.E. and J.O. wrote the manuscript.

Competing interests

The authors declare no competing interests.

Additional information

Supplementary information is available for this paper at https://doi.org/10.1038/s41596-019-0215-x.

Reprints and permissions information is available at www.nature.com/reprints.

Correspondence and requests for materials should be addressed to L.R. or M.E.

Peer review information *Nature Protocols* thanks Hanna Salman and the other, anonymous, reviewer(s) for their contribution to the peer review of this work.

Publisher's note Springer Nature remains neutral with regard to jurisdictional claims in published maps and institutional affiliations.

Received: 23 November 2018; Accepted: 21 June 2019;
Published online: 25 September 2019

Related links
Key reference using this protocol
Robert, L. et al. *Science* **359**, 1283–1286 (2018): http://science.sciencemag.org/content/359/6381/

Key data used in this protocol
Robert, L. et al. *Science* **359**, 1283–1286 (2018): http://science.sciencemag.org/content/359/6381/1283

nature research

Corresponding author(s): Marina Elez, Lydia Robert

Last updated by author(s): May 16, 2019

Reporting Summary

Nature Research wishes to improve the reproducibility of the work that we publish. This form provides structure for consistency and transparency in reporting. For further information on Nature Research policies, see Authors & Referees and the Editorial Policy Checklist.

Statistics

For all statistical analyses, confirm that the following items are present in the figure legend, table legend, main text, or Methods section.

n/a	Confirmed
☒	☐ The exact sample size (*n*) for each experimental group/condition, given as a discrete number and unit of measurement
☒	☐ A statement on whether measurements were taken from distinct samples or whether the same sample was measured repeatedly
☒	☐ The statistical test(s) used AND whether they are one- or two-sided *Only common tests should be described solely by name; describe more complex techniques in the Methods section.*
☒	☐ A description of all covariates tested
☒	☐ A description of any assumptions or corrections, such as tests of normality and adjustment for multiple comparisons
☒	☐ A full description of the statistical parameters including central tendency (e.g. means) or other basic estimates (e.g. regression coefficient) AND variation (e.g. standard deviation) or associated estimates of uncertainty (e.g. confidence intervals)
☒	☐ For null hypothesis testing, the test statistic (e.g. *F*, *t*, *r*) with confidence intervals, effect sizes, degrees of freedom and *P* value noted *Give P values as exact values whenever suitable.*
☒	☐ For Bayesian analysis, information on the choice of priors and Markov chain Monte Carlo settings
☒	☐ For hierarchical and complex designs, identification of the appropriate level for tests and full reporting of outcomes
☒	☐ Estimates of effect sizes (e.g. Cohen's *d*, Pearson's *r*), indicating how they were calculated

Our web collection on statistics for biologists contains articles on many of the points above.

Software and code

Policy information about availability of computer code

Data collection	images were collected using Softworks (commercial software) for µMA experiments and Nis (commercial software) for MV experiments
Data analysis	images were analyzed using BACMMAN (open source software described in Ollion et al. Nature Protocols 2019)

For manuscripts utilizing custom algorithms or software that are central to the research but not yet described in published literature, software must be made available to editors/reviewers. We strongly encourage code deposition in a community repository (e.g. GitHub). See the Nature Research guidelines for submitting code & software for further information.

Data

Policy information about availability of data

All manuscripts must include a data availability statement. This statement should provide the following information, where applicable:

- Accession codes, unique identifiers, or web links for publicly available datasets
- A list of figures that have associated raw data
- A description of any restrictions on data availability

No datasets were generated or analyzed during the current study. Datasets from a related study are archived at Dryad (doi:10.5061/dryad.75625).

Field-specific reporting

Please select the one below that is the best fit for your research. If you are not sure, read the appropriate sections before making your selection.

☒ Life sciences ☐ Behavioural & social sciences ☐ Ecological, evolutionary & environmental sciences

For a reference copy of the document with all sections, see nature.com/documents/nr-reporting-summary-flat.pdf

Life sciences study design

All studies must disclose on these points even when the disclosure is negative.

Sample size	this publication describes a protocol thus there is no life science study design
Data exclusions	this publication describes a protocol thus there is no life science study design
Replication	this publication describes a protocol thus there is no life science study design
Randomization	this publication describes a protocol thus there is no life science study design
Blinding	this publication describes a protocol thus there is no life science study design

Reporting for specific materials, systems and methods

We require information from authors about some types of materials, experimental systems and methods used in many studies. Here, indicate whether each material, system or method listed is relevant to your study. If you are not sure if a list item applies to your research, read the appropriate section before selecting a response.

Materials & experimental systems

n/a	Involved in the study
☒	☐ Antibodies
☒	☐ Eukaryotic cell lines
☒	☐ Palaeontology
☒	☐ Animals and other organisms
☒	☐ Human research participants
☒	☐ Clinical data

Methods

n/a	Involved in the study
☒	☐ ChIP-seq
☒	☐ Flow cytometry
☒	☐ MRI-based neuroimaging